Plasticity of the asialoglycoprotein receptor deciphered by ensemble FRET imaging and single-molecule counting PALM imaging

Malte Renz[a,b], Brian R. Daniels[a], György Vámosi[c], Irwin M. Arias[b], and Jennifer Lippincott-Schwartz[a,1]

[a]Section on Organelle Biology and [b]Unit on Cellular Polarity, The Eunice Kennedy Shriver National Institute of Child Health and Human Development, Cell Biology and Metabolism Branch, National Institutes of Health, Bethesda, MD 20892; and [c]Department of Biophysics and Cell Biology, Medical and Health Science Center, University of Debrecen, H-4012, Debrecen, Hungary

Contributed by Jennifer Lippincott-Schwartz, August 29, 2012 (sent for review May 29, 2012)

The stoichiometry and composition of membrane protein receptors are critical to their function. However, the inability to assess receptor subunit stoichiometry in situ has hampered efforts to relate receptor structures to functional states. Here, we address this problem for the asialoglycoprotein receptor using ensemble FRET imaging, analytical modeling, and single-molecule counting with photoactivated localization microscopy (PALM). We show that the two subunits of asialoglycoprotein receptor [rat hepatic lectin 1 (RHL1) and RHL2] can assemble into both homo- and hetero-oligomeric complexes, displaying three forms with distinct ligand specificities that coexist on the plasma membrane: higher-order homo-oligomers of RHL1, higher-order hetero-oligomers of RHL1 and RHL2 with two-to-one stoichiometry, and the homo-dimer RHL2 with little tendency to further homo-oligomerize. Levels of these complexes can be modulated in the plasma membrane by exogenous ligands. Thus, even a simple two-subunit receptor can exhibit remarkable plasticity in structure, and consequently function, underscoring the importance of deciphering oligomerization in single cells at the single-molecule level.

The plasma membrane contains numerous membrane protein receptors that assemble into homo- and hetero-oligomeric complexes. The precise composition of these receptor complexes is likely to substantially influence activity, highlighting the central importance of visualizing receptor complex stoichiometry. One prototypic plasma membrane receptor is the asialoglycoprotein receptor, which contains two subunits (i.e., subunits 1 and 2) and is involved in receptor-mediated endocytosis in hepatocytes (1). The asialoglycoprotein receptor binds and internalizes diverse classes of desialylated glycoproteins (including asialofetuin) present in the extracellular environment. This activity is crucial for clearance of thrombogenic material (i.e., clotting factors and platelets) under specific pathologic (2) and iatrogenic conditions (3). A key question related to the asialoglycoprotein receptor, in particular, and other multi-subunited receptors on the plasma membrane, in general, is whether the receptors always exist in the same oligomeric configuration in the plasma membrane or whether there is variability in oligomeric assembly and thus function. In the case of the asialoglycoprotein receptor, this question is particularly important, because it is involved in internalizing hundreds of different types of serum glycoproteins. How this process is accomplished by such a two-subunit receptor complex is unclear.

Each of the two subunits of the asialoglycoprotein receptor is a type II membrane protein containing one extracellular carbohydrate recognition domain, a stalk domain, a single-pass transmembrane domain, and an intracellular domain. Only the crystal structure for the carbohydrate recognition domain of receptor subunit 1 exists (4), but the high homology between subunits 1 and 2 suggests that their respective overall structures are similar. The carbohydrate recognition domain is known to mediate binding of terminal Gal and GalNAc residues with high affinity (5). These residues become exposed on many serum glycoproteins when their terminal sialic acid residues are trimmed off by specific enzymes. By recognizing the desialylated glycoproteins (many of which are now inactive) and internalizing them within the cell, the asialoglycoprotein receptor efficiently removes them from the serum. Aside from recognizing desialylated glycoproteins, the asialoglycoprotein receptor has also been reported to bind glycoproteins carrying α2,6-linked sialic acid residues (6) as well as some glycoproteins independently of any specific sugar residues (7).

One way that the asialoglycoprotein receptor could be capable of binding diverse ligands is if it exhibited different oligomeric forms having distinct ligand specificities. So far, efforts at establishing this possibility have proven indecisive. Biochemical approaches have reported vastly different stoichiometries for the asialoglycoprotein receptor, with ratios of subunit 1 to subunit 2 ranging from 2:2 to 8:1 (8–14). Whether these inconsistent results arise from contradictory stoichiometry analysis or the receptor simultaneously assembling into multiple functionally distinct oligomers has remained unclear. However, distinguishing between these possibilities could potentially be addressed by direct visualization of receptor subunit stoichiometry in situ and relating this finding to different functional states.

Here, we take a visualization approach to clarify the plasticity of the asialoglycoprotein receptor. We use advanced spectroscopic tools, including ensemble FRET imaging and single-molecule counting photoactivated localization microscopy (PALM), to test whether cells display different oligomeric forms of the asialoglycoprotein receptor, what the subunit stoichiometries of these forms are, and whether the different oligomeric forms have distinct ligand specificities. We find that the asialoglycoprotein receptor exists in different oligomeric forms, exhibiting structural/functional plasticity. The different forms can be modulated by exogenous ligands, leading to the preferential internalization of one receptor complex over another complex. As exemplified with the asialoglycoprotein receptor, therefore, plasma membrane receptors may be far more plastic and modular systems than previously thought.

Results

Relative Abundances of Receptor Subunits Modulate a Cell's Ability to Bind Different Ligands. To permit spectroscopic analyses of receptor assembly and function in the living cell, we tagged rat asialoglycoprotein receptor subunits [rat hepatic lectin 1 (RHL1) and RHL2] with fluorescent proteins (FPs) and labeled the re-

Author contributions: M.R., I.M.A., and J.L.-S. designed research; M.R. performed research; M.R., B.R.D., and G.V. contributed new reagents/analytic tools; M.R. analyzed data; and M.R. and J.L.-S. wrote the paper.

The authors declare no conflict of interest.

[1]To whom correspondence should be addressed. E-mail: lippincj@mail.nih.gov.

See Author Summary on page 17744 (volume 109, number 44).

This article contains supporting information online at www.pnas.org/lookup/suppl/doi:10.1073/pnas.1211753109/-/DCSupplemental.

ceptor ligands asialofetuin (ASF) and lactoferrin (LTF) (7) with organic dyes. Receptor subunit constructs (FP-RHL1 and FP-RHL2) were expressed in a cell-line model system, normal rat kidney (NRK) cells, which does not express asialoglycoprotein receptor endogenously. Thus, all receptor subunits expressed were FP-labeled and not diluted by an endogenous unlabeled pool. Initially, we tested binding of ASF, a ligand frequently used for asialoglycoprotein receptor studies. When RHL1 or RHL2 is expressed alone, NRK cells did not bind ASF (Fig. 1*A*). Only the coexpression of both receptor subunits resulted in efficient ligand binding (Fig. 1*B* and Fig. S1*D*). In contrast to ASF binding, the expression of RHL1 alone mediated LTF binding, which is shown in Fig. 1*C*. Neither the expression of RHL2 alone nor coexpression of both subunits in comparable amounts led to efficient LTF binding (Fig. 1 *D* and *E*). However, when RHL1 is present at the plasma membrane in high abundance in the presence of RHL2, bound LTF was detectable (Fig. 1*F*).

These experiments suggested that ASF and LTF bind asialoglycoprotein receptor differentially, with each ligand preferring different receptor subunit oligomeric states. Whereas ASF needs to interact with both subunits for it to bind to the receptor, LTF seems to only interact with RHL1. The fact that LTF fails to efficiently bind to cells when RHL1 and RHL2 subunits are equally expressed but does bind when RHL1 is in excess suggests that RHL1 and RHL2 subunits (Fig. S2) assemble into different receptor complexes depending on the amount of subunit being expressed and that the different forms have different ligand specificities.

Differential Homo-Oligomerization of Receptor Subunits Driven by Different Molecular Motifs. Given that differential asialoglycoprotein receptor subunit assembly dictates ligand specificity, we examined whether this finding resulted from the receptor assembling into different homo- or hetero-oligomeric states. To address this problem, we performed FRET analyses (15–17) in live cells expressing single subunits tagged with either Cherry or GFP. In FRET studies, the determination of the relative amount of donor- and acceptor-labeled molecules poses a significant difficulty, because detected donor and acceptor intensities depend not only on the relative concentrations of acceptor and donor dyes but also, instrumental and photophysical parameters (such as excitation intensities, extinction coefficients, fluorescence quantum yields, and detection efficiencies). To overcome this difficulty, we used a GFP-Cherry double construct as a standard, which enabled us to determine the acceptor-to-donor molecule ratios in all doubly labeled samples (18) (*SI Experimental Procedures* and Fig. S3). Also, several semiquantitative FRET methods yield FRET ratios, which in addition to the FRET efficiency, also depend on dye concentrations. In contrast, our FRET analysis (18) based on previous work (19, 20) corrects for spectral spillover between the detection channels and distinct detection efficiencies of the dyes, thus yielding absolute FRET efficiencies, which are crucial for quantitative analysis of receptor subunit assembly. FRET efficiencies were calculated in each pixel of a confocal image and normalized to the FRET efficiency of the GFP-Cherry double construct; thus, FRET efficiencies exceeding the value measured for the GFP-Cherry standard have values greater than 100% on the normalized scale. Only the plasma membrane signal at the rim of cells was analyzed to avoid detection of internal pools. Plotting the FRET efficiency vs. the acceptor-to-donor ratio revealed that the detected FRET values for RHL1 homo-association rose well beyond the positive control and did not plateau (Fig. 2*A*). This unusual behavior suggests that there are many RHL1 subunits assembled into large oligomeric clusters. Only through such homo-oligomeric clustering could the FRET signal continue to increase as the acceptor Cherry-RHL1 levels increase relative to GFP-RHL1. Supporting the notion that RHL1 forms large homo-oligomeric clusters, we found that RHL1 exhibited a highly punctate distribution pattern on the plasma membrane by confocal microscopy (Fig. S1*A*).

To determine what region of the RHL1 subunit is necessary for homo-oligomerization, we deleted the stalk domain (RHL1Δc), which is proposed to mediate a tight coiled-coil interaction (21). This deletion led to normalized FRET efficiencies of about 25% either between WT and mutant RHL1Δc or among mutant RHL1Δc (Fig. 2*B* and Fig. S4). The FRET efficiency did not increase as the acceptor-to-donor ratio increased, indicating that homo-oligomerization into large clusters did not occur. FRET measurements of RHL1 mutants comprising only the intracellular and transmembrane domains (RHL1TMs) also showed that these domains did not significantly homo-oligomerize (Fig. 2*B*). Hence, the stalk domain is the major driving force for RHL1 homo-oligomerization.

In contrast to RHL1, RHL2, when expressed alone, showed a homogeneous distribution at the plasma membrane by confocal microscopy (Fig. S1*B*). Detected normalized FRET efficiencies were distinctly lower than for RHL1, and they leveled off at 40% at an acceptor-to-donor ratio of about 1.0 (Fig. 2*C*). This finding suggested that RHL2 subunits exist primarily as homo-dimers in the plasma membrane with only a few oligomeric clusters. Deletion of all extracellular domains resulted in a FRET curve similar to the curve of the WT RHL2, suggesting that the RHL2 self-association is mediated mainly through the cytoplasmic and transmembrane domains (Fig. 2*C*). Thus, despite the high sequence homology between RHL1 and RHL2 (Fig. S2), our ensemble FRET measurements revealed distinct differences in the extent of RHL1–RHL1 and RHL2–RHL2 homo-oligomerization. Whereas RHL1 underwent extensive homo-oligomerization and clustering mediated by its stalk domain, RHL2 did not, and instead, RHL2 distributed mainly as homo-dimers in the plasma membrane.

Receptor Subunit 2 Limits Receptor Subunit 1 Homo-Association. We next investigated how self-association of RHL1 is affected by the presence of RHL2. To analyze this problem, we labeled RHL2 with PA-Cherry and looked to see if its expression affected the FRET signal from oligomers containing GFP-RHL1 and Cherry-RHL1. Before photoactivation, the PA-Cherry construct should not interfere with the energy transfer between GFP-RHL1 and Cherry-RHL1 in such oligomers unless the presence of RHL2 changes RHL1 self-association. Photoactivation, however, should result in a distinct increase in red fluorescence and thus FRET efficiency if PA-Cherry-RHL2 assembles into the GFP-RHL1 and Cherry-RHL1 homo-oligomers (Fig. S5 has a more detailed description of this use of PA-Cherry as a photoactivatable FRET probe). We began by examining RHL1 self-association in the presence and absence of RHL2 (Fig. 2*D*). Notably, in the presence of RHL2, normalized FRET efficiencies for RHL1–RHL1 interactions decreased before photoactivation of PA-Cherry. This result suggested that the presence of RHL2 interferes with the extent of RHL1 homo-oligomerization. RHL2 binding to RHL1 presumably competes with other RHL1 molecules and limits RHL1 homo-oligomerization. When we performed a similar FRET analysis looking at how RHL2 self-association is affected by the presence of RHL1, we found that it remained unchanged (Fig. 2*E*). Thus, whereas homo-oligomeric interactions between RHL1 molecules are affected by RHL2 expression, the reverse is not true, and RHL2 remained homo-dimeric.

Asymmetric Receptor Subunit Hetero-Oligomerization. The above results suggest that hetero-oligomers of RHL1 and RHL2 exist. To gain insight into the stoichiometric composition of these hetero-oligomers, we again used ensemble FRET analysis. If RHL1 and RHL2 assembled symmetrically into hetero-oligomers (i.e., 1:1 or 2:2, etc.), then normalized FRET efficiency curves are expected to coincide, irrespective of whether RHL1 or RHL2 serves as donor or acceptor. Significantly, this result was not observed.

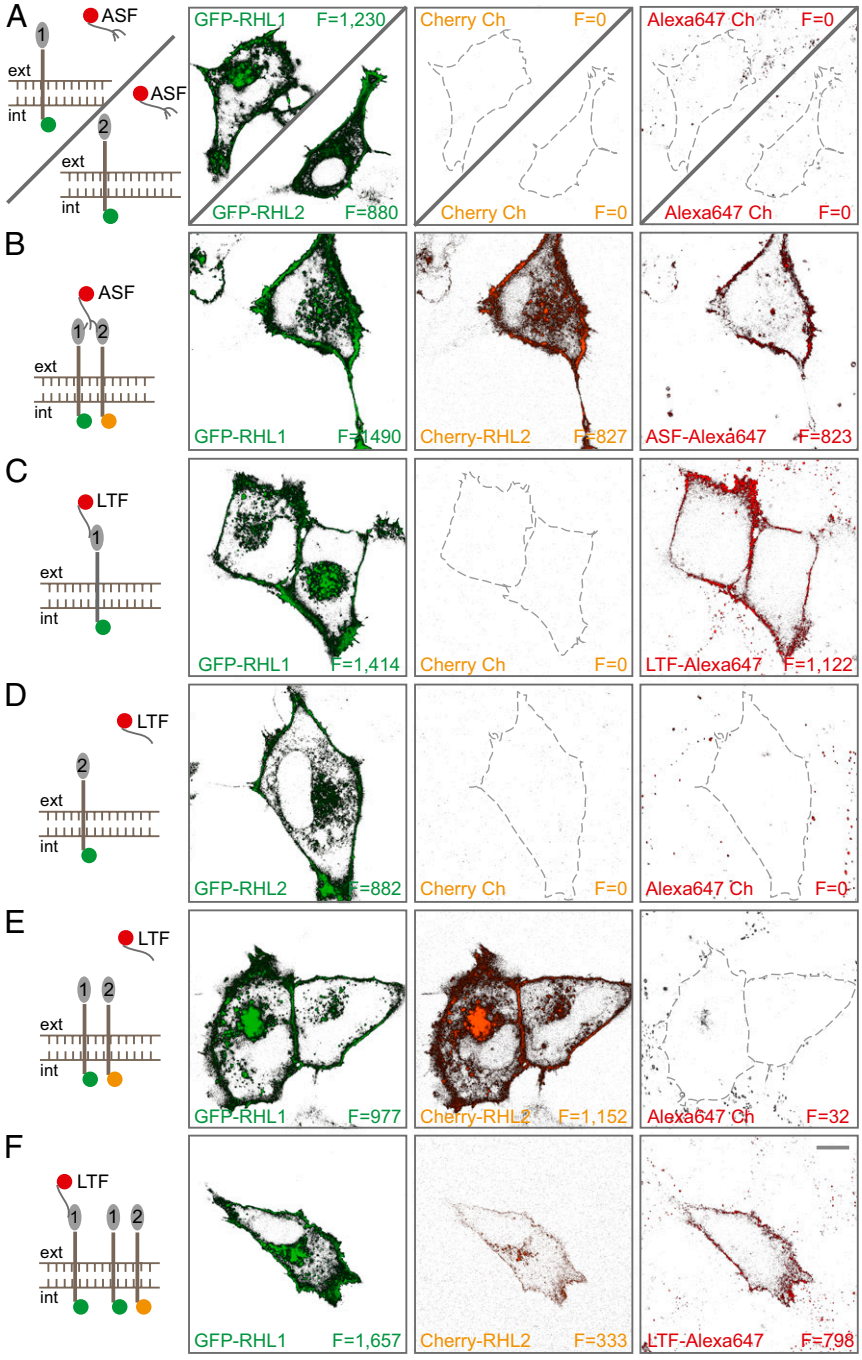

Fig. 1. Differential asialoglycoprotein receptor subunit assembly dictates ligand specificity. NRK cells expressing different combinations of GFP-RHL1, GFP-RHL2, and/or Cherry-RHL2 were examined for their ability to bind Alexa647-labeled ASF or Alexa647-LTF. Green, red, and far-red channels are displayed. Mean fluorescence intensity (F) was calculated by integrating over the pixels corresponding to the plasma membrane. (*A*) Cells expressing either RHL1 or RHL2 alone did not bind ASF. (*B*) Coexpression of RHL1 and RHL2 resulted in efficient ASF binding. (*C*) RHL1 expression alone resulted in efficient LTF binding. (*D*) RHL2 expression alone did not result in efficient LTF binding. (*E*) Expressing both subunits in comparable amounts did not lead to LTF binding. (*F*) RHL1 expression at high levels relative to RHL2 led to detectable LTF binding. (Scale bar: 10 μm.)

Labeling RHL1 with GFP and RHL2 with Cherry yielded a steeply increasing FRET curve that leveled off at low acceptor-to-donor ratios (Fig. 3*A*). The reverse labeling, by contrast, yielded an almost linearly increasing FRET curve that plateaued only at higher acceptor-to-donor ratios (Fig. 3*B*). This finding indicated that the stoichiometry of subunits RHL1 and RHL2 in receptors was not symmetric. The major determinant of RHL1 and RHL2 hetero-oligomerization resided in the stalk domains of these subunits, since the normalized FRET efficiency between mutant RHL1Δ and RHL2 was always only about 20% (Fig. S6*A*) compared with the full-length subunits having 80–120% normalized FRET efficiency at high acceptor-to-donor ratios (Fig. 3 *A* and *B*).

The results of our FRET analysis for homo- and hetero-oligomers allowed us to speculate on a possible stoichiometry of the receptor. Given that RHL1 has a higher tendency to form

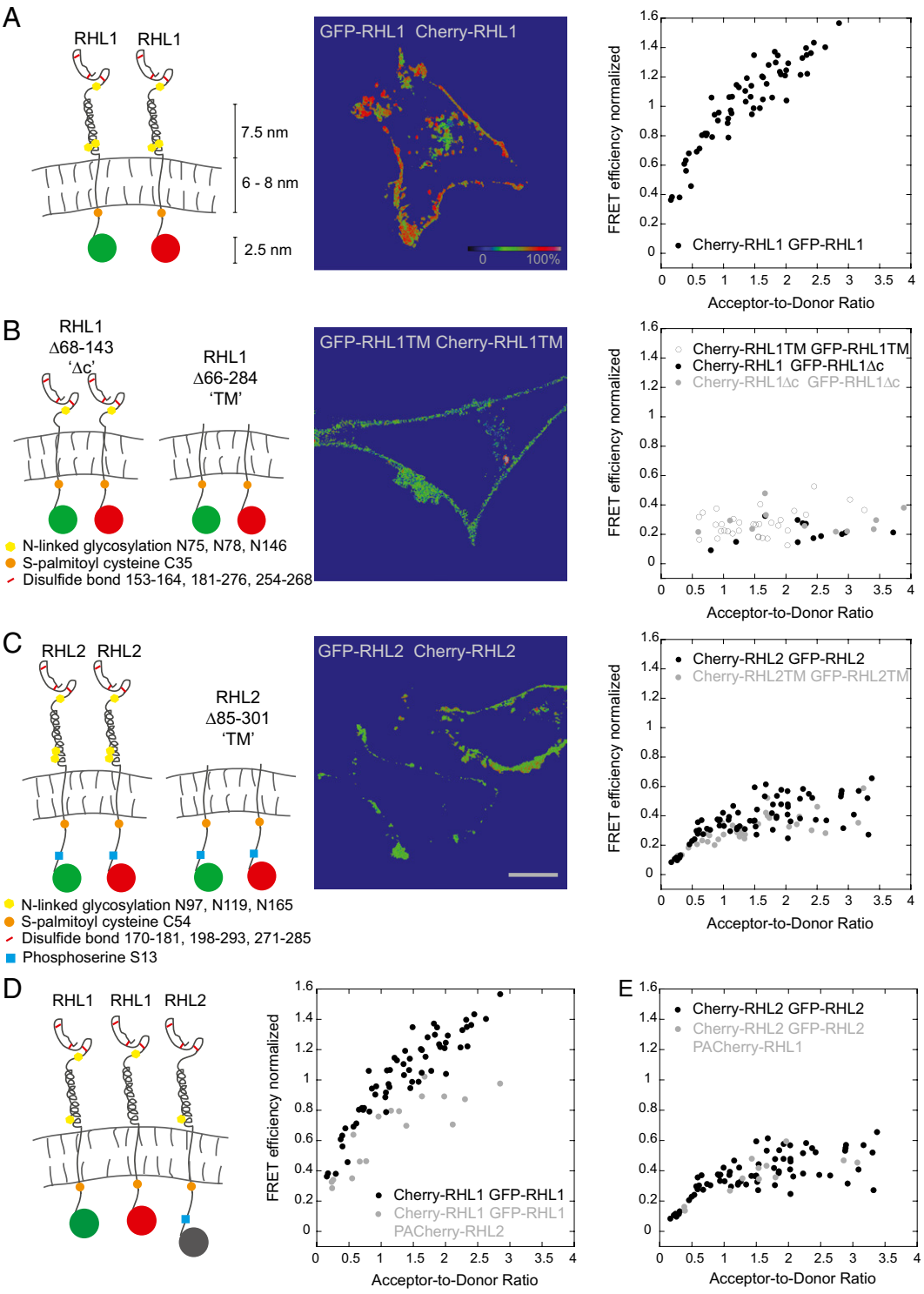

Fig. 2. Ensemble FRET analyses show distinct homo-oligomerization of RHL1 and RHL2 driven by different molecular motifs. The cartoons depict the studied subunits or their mutant forms. The images display color-coded FRET values in each pixel. The color-coded scale bar is for normalized mean FRET efficiencies. (Scale bar: *A–C*, 10 μm.) In the graphs, mean normalized FRET efficiencies integrated over the pixels corresponding to the plasma membrane were plotted vs. the acceptor-to-donor ratio. (*A*) Homo-oligomerization of RHL1. Plotting the FRET efficiency vs. the acceptor-to-donor ratio revealed that the detected FRET values for RHL1 homo-association rose well beyond the positive control and did not plateau, indicating that RHL1 homo-associates into large clusters. (*B*) Deletion of RHL1's stalk domain (RHL1Δc) and all external domains (RHL1TM) led to a normalized FRET efficiency of about 25% between WT and mutant RHL1 forms and among the mutants. This finding suggests that the major driving force for RHL1 homo-oligomerization is the stalk domain. (*C*) Homo-oligomerization of RHL2. RHL2 forms homo-dimers and not higher-order oligomers. Deletion of all external domains of RHL2 did not change the normalized FRET efficiencies. Thus, RHL2 homo-oligomerization is mainly determined by transmembrane and intracellular domains. (*D*) Self-association of RHL1 decreases in the presence of RHL2. RHL1 homo-association is shown side by side in the presence and absence of PA-Cherry–labeled RHL2. FRET between RHL1 molecules was measured before activation of PA-Cherry. (*E*) Self-association of RHL2 is unchanged in the presence of RHL1. RHL2 self-association is shown side by side in the presence and absence of PA-Cherry–labeled RHL1. FRET between RHL2 molecules was measured before activation of PA-Cherry.

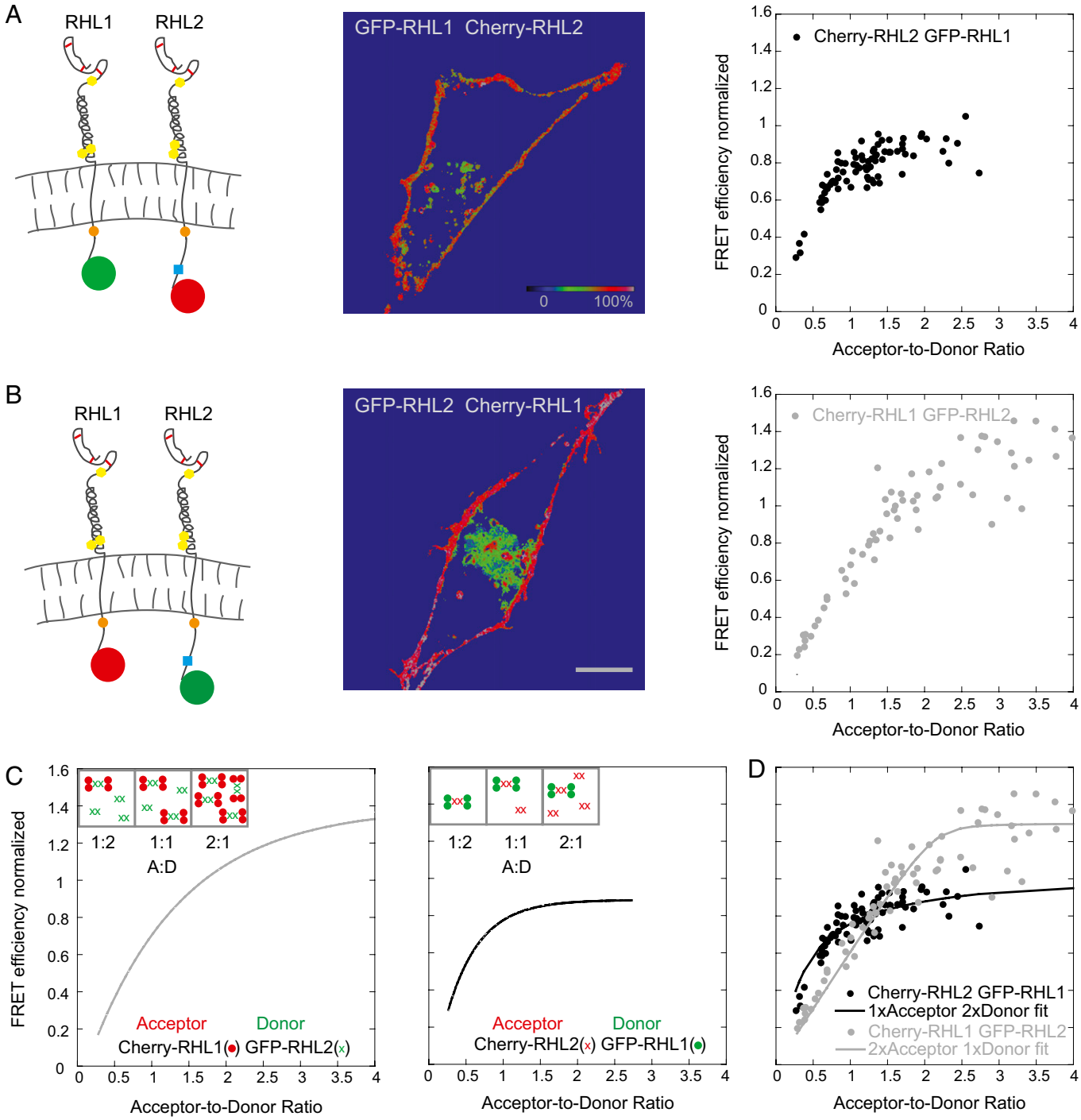

Fig. 3. Ensemble FRET analyses reveal an asymmetric receptor subunit assembly of the asialoglycoprotein receptor. (*A*) FRET efficiencies between GFP-labeled RHL1 (donor) and Cherry-labeled RHL2 (acceptor). The detected FRET curve exhibits a steep increase followed by an early plateau. The cartoons in *A* and *B* depict the studied RHL1 and RHL2 labeled with donor or acceptor, respectively. The images display the color-coded FRET values in each pixel. Mean FRET efficiency integrated over the pixels showing the plasma membrane was plotted vs. the acceptor-to-donor ratio. The color-coded scale bar is for normalized mean FRET efficiencies. (Scale bar: *A* and *B*, 10 μm.) (*B*) FRET efficiencies of Cherry-labeled RHL1 and GFP-labeled RHL2. The FRET curve exhibits an almost linear increase and plateaus only at a high acceptor-to-donor ratio. (*C*) Schematic explanation for the detected nonidentical FRET curves of RHL1/RHL2 hetero-oligomerization. *Insets* show the simplest explanation of an asymmetric receptor subunit hetero-oligomerization: a stoichiometric distribution of two RHL1 dimers to one RHL2 dimer in a receptor complex. Hypothesized FRET curves consistent with this explanation that match the experimental data in *A* and *B* are shown in the graphs. (*D*) Analytical model for the schematic explanation above (*SI Experimental Procedures*). The model calculations showed that the experimental data of *A* and *B* (shown as gray and black dots, respectively) can be fit (gray and black lines, respectively) to a receptor subunit stoichiometry of 2:1 (RHL1:RHL2) and ruled out a symmetric receptor subunit hetero-oligomerization.

oligomers than RHL2, which forms predominantly homo-dimers (Fig. 2), we assumed the simplest asymmetric receptor subunit composition of two RHL1 homo-dimers to every one RHL2 homo-dimer. In this scenario, when RHL1 is labeled with Cherry and forms acceptor homo-dimers that associate with RHL2 homo-dimers with a stoichiometry of 2:1 (shown schematically in

Fig. 3*C*), significant portions of RHL2 homo-dimeric donors are free without any acceptor and cannot transfer energy at an acceptor-to-donor ratio of 1:2. As the molar acceptor-to-donor ratio rises (i.e., A:D as 1:1 and 2:1), an increasing number of donors has an acceptor dimer and can transfer energy, resulting in an almost linear increase in FRET that is eventually higher than the energy transfer efficiency between the 1:1 GFP-Cherry positive control. Changing colors, two donor dimers have, on average, one acceptor dimer already at an acceptor-to-donor ratio of 1:2, explaining the steep initial increase of FRET efficiency. Because the binding sites on the donor are occupied, a further increase in the acceptor-to-donor ratio results only in free acceptor dimers that do not contribute to FRET. Therefore, the FRET curve plateaus early and shows no additional rise.

We formulated an analytical model based on mass action to test the above scheme more rigorously (*SI Experimental Procedures*). The model simulations showed that the experimental data could be fit to a receptor subunit stoichiometry of 2:1 (RHL1:RHL2) (Fig. 3*D*) and ruled out a symmetric receptor subunit composition. Taking into account that RHL2 likely exists in a dimeric state in both the presence and absence of RHL1 (Fig. 2*E*), this 2:1 stoichiometry suggests a basic building block for the hetero-oligomers comprising 2× RHL1 homo-dimers and 1× RHL2 homo-dimer. These receptor cores may form larger hetero-oligomers as suggested by the punctate plasma membrane distribution of coexpressed RHL1 and RHL2 (Fig. S1 *C* and *D*).

Single-Molecule Counting PALM for Assessing Relative Expression and Stoichiometries. To obtain direct visualization of receptor composition and stoichiometry, we turned to photoactivated localization microscopy (PALM) (22). In this single molecule-based imaging technique, repeated activation and sampling of individual molecules permit densely expressed fluorescent proteins to be resolved in time. So far, PALM has been primarily used as a tool for obtaining superresolution images, with single molecules used as mere image constituents, rather than counting individual molecules. We reasoned that, using the inherent numerical information of PALM for single-molecule counting, it should be possible to obtain quantitative information about receptor subunit assemblies, even in membrane areas of high receptor density. Previous molecule counting approaches, such as stepwise photobleaching, are intensity-based and only count up to four molecules of one type in a diffraction-limited spot (i.e., ∼200 nm diameter) (23). They, thus, cannot examine the assembly of two different subunits or protein subunit distribution at physiological expression levels on the plasma membrane, where hundreds of copies of a particular receptor often exist within a diffraction-limited spot.

Using PALM, we aimed to analyze the stoichiometry of RHL1 and RHL2 labeled with two different colors simultaneously in the same specimen, counting tens of thousands of molecules to define receptor oligomerization state in its physiological context on the plasma membrane of cells. We began by testing our ability to reproducibly count two different photoactivatable fluorophores attached to the same protein in a 1:1 ratio (Fig. S7). As photoactivatable fluorophores, we used PA-GFP and PA-Cherry, which are irreversible dark-to-bright photoactivatable fluorescent proteins (24, 25). This strategy allowed us to count a given population of molecules two times—first in green and then in red. By coupling the genetic information of a green and a red PA-FP, internal rulers are created that will be expressed in a fixed and known relative amount of 1:1. Measuring different cells expressing this construct, we tested if a specific ratio could be stably reproduced, which indicated that single-molecule counting with PALM is possible.

We developed an efficient, sequential, two-color PALM imaging regimen utilizing differential photoactivatability of the different PA-FPs (Figs. S8 and S9 and Movie S1). Criteria to determine the identity of a single molecular event were also defined (Figs. S10, S11, and S12 and Movies S2 and S3). Applying the imaging and analysis regimen to the PA-GFP-PA-Cherry double construct (Fig. 4*A*), we were able to stably reproduce a specific red-to-green ratio in different cells expressing the test construct in different absolute amounts and thus, show that single-molecule counting with PALM is possible.

The use of spectrally distinct fluorophores in this manner provides internal rulers, yielding information as to how efficiently these fluorophores can be detected in relation to one another (Fig. 4*B*). It, thus, should provide information about the relative expression of two proteins of interest in a given membrane area. To test, probes of known stoichiometries were constructed comprising different copy numbers of PA-GFP and PA-Cherry. As shown in Fig. 4*C*, single-molecule counting yielded the actual stoichiometries. Red and green single-molecule counts scaled linearly relative to each other in this cell-based dilution series.

Determination of Receptor Subunit Stoichiometry in Situ at the Single-Molecule Level. Having shown that single-molecule counting PALM is possible and can be used to assess the relative amount of two spectrally distinct PA-FPs, we applied single-molecule counting to address asialoglycoprotein receptor oligomerization. RHL1 homo-oligomerization was analyzed (Fig. 4 *D* and *F*). We determined the molecular density, the relative expression of red and green molecules in a given membrane area, and the relative expression within protein clusters. The chance to be assembled in such a homo-oligomeric cluster is governed by the relative amount of red- and green-labeled molecules present in a given membrane area. Thus, the average red-to-green ratio within clusters equals the overall ratio.

Addressing next hetero-oligomerization, we found in the cell exemplarily depicted in Fig. 4*E* the same molecular density in an equal-sized membrane region and the same relative overall expression of red and green molecules as in the cell expressing just the RHL1. Since protein interactions may depend on the relative amount of interacting partners and the analytical readout certainly depends on the detected numerical proportion and protein density, these two cells shown here are directly comparable. In contrast to RHL1 homo-oligomers, the hetero-oligomer of RHL1 and RHL2 shows a red-to-green ratio distinct from the overall relative expression. RHL1 is apparently more abundant in detected protein clusters, while there are more free RHL2 subunits present outside the clusters, revealing an asymmetric receptor subunit assembly that approximates two RHL1 to every one RHL2 in a cluster. Thus, single-molecule counting PALM visualized RHL1 homo-association and RHL1/RHL2 hetero-association into distinct clusters that preserve a 2:1 stoichiometry in the presence of free RHL2 subunits, thereby confirming our ensemble FRET data on the single-molecule level. Having shown that single-molecule counting PALM is possible and can be used to assess the relative amount of spectrally distinct fluorescent proteins, it is critical to state that numbers of detected fluorescent molecules should not be interpreted simply as numbers of molecules expressed, primarily because not all fluorophores photoactivate and become fluorescent (26).

Ligand-Induced Shift in the Distribution of Different Coexisting Receptor Subunit Oligomers at the Plasma Membrane. We next tested if the presence of exogenous ligand modulates the distribution of the coexistent distinct homo- and hetero-oligomeric receptor subunit assemblies at the plasma membrane of a single cell. We reasoned that the addition of ligands specific to the different coexisting receptor subunit oligomers should lead to a predominant internalization of one oligomeric state over another state from the plasma membrane and thereby, shift the steady-state distribution of the distinct oligomeric states (Fig. 5*C*). To monitor this shift in one and the same live cell over time, we turned again to ensemble FRET analyses between RHL1 labeled with GFP and RHL2 labeled with Cherry and monitored the development of

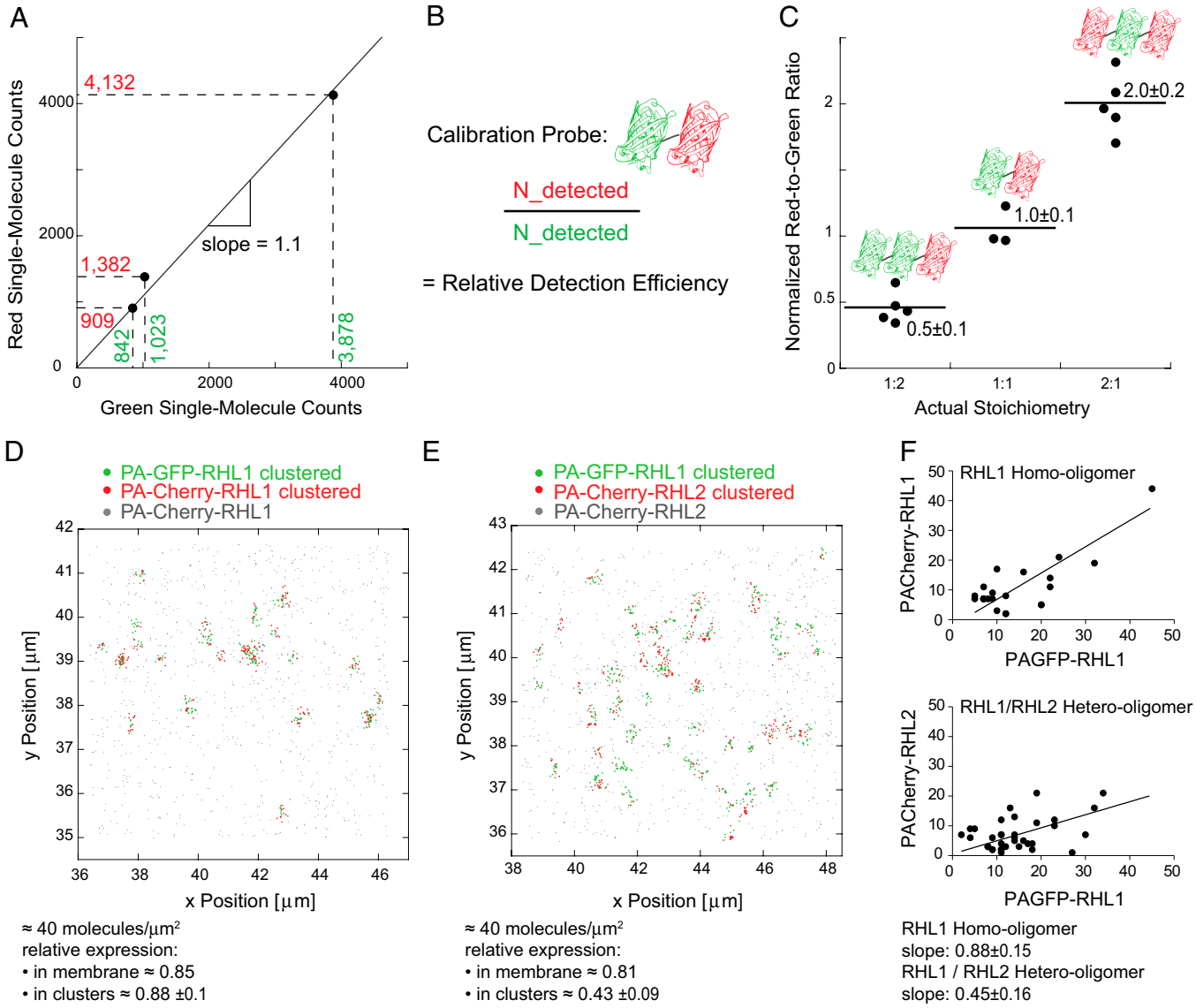

Fig. 4. Single-molecule counting PALM visualizes an asymmetric receptor subunit assembly of asialoglycoprotein receptor on the single-molecule level. (*A*) Single-molecule counting PALM was capable of stably reproducing a specific red-to-green ratio in different cells expressing the vesicular stomatitis virus glycoprotein-PA-GFP-PA-Cherry double construct in different absolute amounts. (*B*) Strategy for determining the relative detection efficiency of PA-GFP and PA-Cherry using a calibration probe. (*C*) Applying single-molecule counting PALM to cells expressing vesicular stomatitis virus glycoprotein constructs containing PA-GFP and PA-Cherry in differing amounts permits assessment of the correct stoichiometry of the constructs. Three constructs having the following ratios of PA-Cherry and PA-GFP were assessed: 1 PA-Cherry:2 PA-GFP; 1 PA-Cherry:1 PA-GFP; and 2 PA-Cherry:1 PA-GFP. The red-to-green ratio in each cell expressing the given constructs was determined and normalized to the relative detection efficiency. (*D*) Coexpression of RHL1 labeled with PA-GFP and PA-Cherry. Applying single-molecule counting PALM, we detected 40 molecules/μm^2 and a relative red-to-green ratio of 0.85 in a membrane area of 36 μm^2. The relative red-to-green ratio within an RHL1 homo-oligomeric cluster was 0.88 ± 0.1. (*E*) Coexpression of PA-GFP-RHL1 and PA-Cherry-RHL2. Applying single-molecule counting PALM, we detected 40 molecules/μm^2 and a relative red-to-green ratio of 0.81 in a membrane area of 36 μm^2. The relative red-to-green ratio of 0.43 ± 0.09 within a hetero-oligomeric cluster, however, deviated significantly from the relative overall expression. RHL1 was more abundant inside the clusters, indicating an asymmetric receptor assembly that approximates a stoichiometry of two RHL1 to every one RHL2 in a cluster. (*F*) Plotting the detected number of red and green molecules inside the homo- and hetero-oligomeric clusters can be fit to straight lines with a slope of 0.88 ± 0.15 for the RHL1 homo-oligomers as displayed in *D* and 0.45 ± 0.16 for the RHL1/RHL2 hetero-oligomers as shown in *E*. The slope of the line fit gives an estimate for the average stoichiometry within a cluster and coincides with the red-to-green ratio within the homo- and hetero-oligomeric clusters, respectively.

detected FRET efficiencies after the addition of exogenous ligand. We hypothesized that, after addition of asialofetuin, the hetero-oligomeric receptor states should be internalized, leaving behind the donor-only GFP-labeled RHL1 homo-oligomers, which results in a stepwise decrease in detected FRET efficiency over time. In fact, we recorded a 6.5% decrease in normalized FRET over 15 min. The addition of lactoferrin, however, should bind and deplete the homo-oligomeric receptor states from the plasma membrane by internalization and thus, increase detected FRET efficiencies. An increase in FRET of 10% over 20 min was detected under these conditions. No change in FRET over the same time period occurred when no ligand was added. These data not only support the coexistence of different homo- and hetero-oligomeric receptor states at the plasma membrane and their differential functionality but also show that the structural/functional plasticity of the asialoglycoprotein receptor can be modulated by exogenous ligands and that thereby one oligomeric population can be selectively down-regulated.

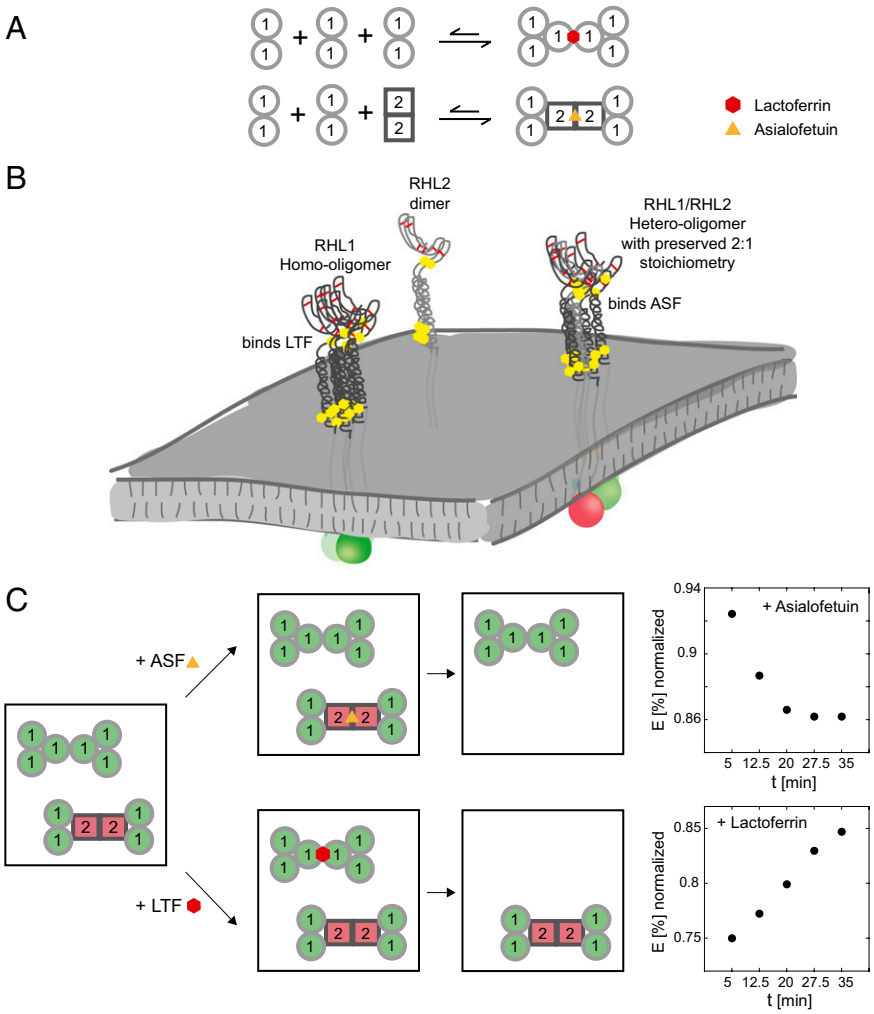

Fig. 5. Assembly of asialoglycoprotein receptor into different homo- and hetero-oligomeric states with distinct ligand specificities defines receptor plasticity and can be modulated further by exogenous ligands. (*A*) The assembly of the asialoglycoprotein receptor on the plasma membrane can be pictured as a modular system. Because of its high tendency to homo-associate, RHL1 will form homo-oligomers that can bind lactoferrin. When RHL2 homo-dimers are present at the plasma membrane, they associate with RHL1 mediated through the stalk domain and weaken the tendency of RHL1 to self-associate. RHL1 and RHL2 form hetero-oligomers comprising receptor cores of two RHL1 homo-dimers and one RHL2 homo-dimer. Both the homo-oligomeric complexes of RHL1 and the hetero-oligomeric complexes can further associate to higher-order oligomers that, in the case of the hetero-oligomer, preserve a 2:1 stoichiometry of RHL1:RHL2. (*B*) Differential oligomerization driven by different molecular motifs and different subunit abundances leads to the coexistence of different oligomers with distinct ligand specificities at the plasma membrane. (*C*) The steady-state equilibrium of the distinct coexistent homo- and hetero-oligomeric receptor states can be shifted by exogenous ligand. When asialofetuin is added, it binds to the hetero-oligomeric complexes and leads to their internalization, leaving behind RHL1 homo-oligomers. Because RHL1 is labeled with GFP, donor-only complexes will be enriched at the plasma membrane, which results in a decrease in detected normalized FRET efficiencies of RHL1 labeled with GFP and RHL2 labeled with Cherry. The addition of lactoferrin, however, leads to the internalization of donor-only RHL1 homo-oligomers, leaving behind the hetero-oligomeric complexes and thus results in an increase in detected FRET efficiencies.

Discussion

The above ensemble FRET and single-molecule counting PALM data suggest a probability hierarchy of oligomerization of the asialoglycoprotein receptor driven by distinct molecular motifs. This finding sets the molecular basis of coexistent distinct receptor subunit oligomers at the plasma membrane (Fig. 5). As exemplified, the tendency of the subunits to oligomerize and their differences in relative expression are sufficient determinants for differential receptor subunit assembly that, in turn, dictates ligand specificity and thereby, defines receptor plasticity. Because of its high tendency to homo-associate, RHL1 will form homo-oligomers that can bind lactoferrin. When RHL2 dimers are present at the plasma membrane, they associate with RHL1 mediated by the stalk domains and weaken the tendency of RHL1 to self-associate. RHL1 and RHL2 form hetero-oligomers that can assemble into higher-order oligomers, comprising receptor cores of two RHL1 homo-dimers and one RHL2 homodimer, thereby preserving a 2:1 stoichiometry. These hetero-oligomeric receptors exhibit ligand specificity distinct from RHL1 homo-oligomers: they cannot bind lactoferrin but do bind asialofetuin. When RHL1 is expressed in excess relative to RHL2, RHL1 readily forms homo-oligomers that again are able to bind lactoferrin. The detected structural/functional plasticity of the asialoglycoprotein receptor can be modulated further by exogenous ligands, leading to a shift in steady-state distribution of the different receptor subunit oligomers. Thus, a simple two-subunit membrane protein receptor like the asialoglycoprotein receptor can exhibit great structural/functional plasticity.

The asialoglycoprotein receptor is a highly abundant receptor system with up to 500,000 binding sites (27) at the basolateral cell surface of hepatocytes facing the blood stream. The coexistence of distinct oligomerization states of the asialoglycoprotein receptor may provide a versatile means to efficiently bind different gly-

coproteins. This result is likely to serve as a robust clearance mechanism for large amounts of desialylated glycoproteins of diverse types that suddenly arise, for instance, in septic conditions. The plastic modularity of the receptor system, however, may allow rapid shifts in specificity by changing the relative abundance of its different oligomeric states. This may account for the rapid depletion of specific glycoproteins and potentially, even platelets, which are seen under specific pathologic conditions. In turn, the variety of potential ligands for asialoglycoprotein receptor and the propensity of its subunits to form distinct oligomers may explain previous inconsistent results, and underscores the importance of deciphering oligomerization in the single cell and on the single-molecule level. We anticipate that the spectroscopic tools presented here will help decipher plasticity in stoichiometry and function of other receptor systems in the single cell and on the single-molecule level.

Experimental Procedures

Mammalian Plasmids, Cell Culture, and Sample Preparation. Detailed information about cloning of WT rat asialoglycoprotein receptor subunits (NM_012503 and NM_017189) and their various mutants as well as construction of the various fluorescent protein chimeras and cell culture is in *SI Experimental Procedures*.

Confocal Microscopy and Determination of Pixel-by-Pixel FRET Efficiencies. Cell imaging was performed on a Zeiss LSM510 confocal laser scanning microscope equipped with a 63× Plan Apochromat N.A. 1.4 oil immersion objective. FRET efficiency (E) and acceptor-to-donor ratio were determined as previously described (18). A detailed description of FRET measurements is in *SI Experimental Procedures*.

Mathematical Modeling. To model FRET efficiency (E) as determined by the fraction of donor (D) that is part of a complex and therefore, can be quenched, we considered a reaction equilibrium described by the law of mass action. A detailed description of the analytical modeling is in *SI Experimental Procedures*.

Photoactivated Localization Microscopy. Detailed information on single-molecule counting PALM is in *SI Experimental Procedures*.

ACKNOWLEDGMENTS. We thank Dr. Ramanujan Hegde, Dr. Alexander Gansen, and Dr. Christian Wunder for critical discussion and reading of the manuscript. M.R. was supported by German Research Foundation Fellowship DFG 2893/1-1 and the Charles Trey, MD Memorial Postdoctoral Research Award from the American Liver Foundation. G.V. was supported by the Hungarian Scientific Research Foundation OTKA K77600 and TÁMOP-4.2.1/B-09/1/KONV-2010-0007 cofinanced by the European Social Fund and European Regional Development Fund.

1. Hudgin RL, Pricer WE, Jr., Ashwell G, Stockert RJ, Morell AG (1974) The isolation and properties of a rabbit liver binding protein specific for asialoglycoproteins. *J Biol Chem* 249:5536–5543.
2. Grewal PK, et al. (2008) The Ashwell receptor mitigates the lethal coagulopathy of sepsis. *Nat Med* 14:648–655.
3. Rumjantseva V, et al. (2009) Dual roles for hepatic lectin receptors in the clearance of chilled platelets. *Nat Med* 15:1273–1280.
4. Meier M, Bider MD, Malashkevich VN, Spiess M, Burkhard P (2000) Crystal structure of the carbohydrate recognition domain of the H1 subunit of the asialoglycoprotein receptor. *J Mol Biol* 300:857–865.
5. Ashwell G, Harford J (1982) Carbohydrate-specific receptors of the liver. *Annu Rev Biochem* 51:531–554.
6. Park EI, Mi Y, Unverzagt C, Gabius HJ, Baenziger JU (2005) The asialoglycoprotein receptor clears glycoconjugates terminating with sialic acid alpha 2,6GalNAc. *Proc Natl Acad Sci USA* 102:17125–17129.
7. Bennatt DJ, Ling YY, McAbee DD (1997) Isolated rat hepatocytes bind lactoferrins by the RHL-1 subunit of the asialoglycoprotein receptor in a galactose-independent manner. *Biochemistry* 36:8367–8376.
8. Steer CJ, Kempner ES, Ashwell G (1981) Molecular size of the hepatic receptor for asialoglycoproteins determined in situ by radiation inactivation. *J Biol Chem* 256: 5851–5856.
9. Halberg DF, et al. (1987) Major and minor forms of the rat liver asialoglycoprotein receptor are independent galactose-binding proteins. Primary structure and glycosylation heterogeneity of minor receptor forms. *J Biol Chem* 262:9828–9838.
10. Sawyer JT, Sanford JP, Doyle D (1988) Identification of a complex of the three forms of the rat liver asialoglycoprotein receptor. *J Biol Chem* 263:10534–10538.
11. Herzig MC, Weigel PH (1989) Synthesis and characterization of N-hydroxysuccinimide ester chemical affinity derivatives of asialoorosomucoid that covalently cross-link to galactosyl receptors on isolated rat hepatocytes. *Biochemistry* 28:600–610.
12. Henis YI, Katzir Z, Shia MA, Lodish HF (1990) Oligomeric structure of the human asialoglycoprotein receptor: Nature and stoichiometry of mutual complexes containing H1 and H2 polypeptides assessed by fluorescence photobleaching recovery. *J Cell Biol* 111:1409–1418.
13. Bider MD, Wahlberg JM, Kammerer RA, Spiess M (1996) The oligomerization domain of the asialoglycoprotein receptor preferentially forms 2:2 heterotetramers in vitro. *J Biol Chem* 271:31996–32001.
14. Ramadugu SK, Chung YH, Fuentes EJ, Rice KG, Margulis CJ (2010) In silico prediction of the 3D structure of trimeric asialoglycoprotein receptor bound to triantennary oligosaccharide. *J Am Chem Soc* 132:9087–9095.
15. Förster T (1948) Zwischenmolekulare Energiewanderung und Fluoreszenz. *Ann Phys* 437:55–75.
16. Stryer L, Haugland RP (1967) Energy transfer: A spectroscopic ruler. *Proc Natl Acad Sci USA* 58:719–726.
17. Clegg RM (1995) Fluorescence resonance energy transfer. *Curr Opin Biotechnol* 6: 103–110.
18. Vámosi G, et al. (2008) Conformation of the c-Fos/c-Jun complex in vivo: A combined FRET, FCCS, and MD-modeling study. *Biophys J* 94:2859–2868.
19. Trón L, et al. (1984) Flow cytometric measurement of fluorescence resonance energy transfer on cell surfaces. Quantitative evaluation of the transfer efficiency on a cell-by-cell basis. *Biophys J* 45:939–946.
20. Sebestyén Z, et al. (2002) Long wavelength fluorophores and cell-by-cell correction for autofluorescence significantly improves the accuracy of flow cytometric energy transfer measurements on a dual-laser benchtop flow cytometer. *Cytometry* 48:124–135.
21. Beavil AJ, Edmeades RL, Gould HJ, Sutton BJ (1992) Alpha-helical coiled-coil stalks in the low-affinity receptor for IgE (Fc epsilon RII/CD23) and related C-type lectins. *Proc Natl Acad Sci USA* 89:753–757.
22. Betzig E, et al. (2006) Imaging intracellular fluorescent proteins at nanometer resolution. *Science* 313:1642–1645.
23. Ulbrich MH, Isacoff EY (2007) Subunit counting in membrane-bound proteins. *Nat Methods* 4:319–321.
24. Patterson GH, Lippincott-Schwartz J (2002) A photoactivatable GFP for selective photolabeling of proteins and cells. *Science* 297:1873–1877.
25. Subach FV, et al. (2009) Photoactivatable mCherry for high-resolution two-color fluorescence microscopy. *Nat Methods* 6:153–159.
26. Renz M, Lippincott-Schwartz J (2011) Single-molecule counting with PALM. *Biophys J*, 10.1016/j.bpj.2010.12.2106.
27. Schwartz AL, Rup D, Lodish HF (1980) Difficulties in the quantification of asialoglycoprotein receptors on the rat hepatocyte. *J Biol Chem* 255:9033–9036.